Journal of Solid Mechanics Vol. 13, No. 3 (2021) pp. 286-296
DOI: 10.22034/jsm.2020.1878636.1496

Study on Vibration Band Gap Characteristics of a Branched Shape Periodic Structure Using the GDQR

M. Hajhosseini *, A. Abshahi

Department of Mechanical Engineering, Vali-e-Asr University of Rafsanjan, Rafsanjan, Iran

Received 26 March 2021; accepted 27 May 2021

ABSTRACT

In this study, a new periodic structure with special vibration band gap properties is introduced. This structure consists of a main beam and several cantilever beam elements connected to this main beam in the branched shape. Two models with different number of beam elements and geometrical parameters are considered for this periodic structure. The transverse vibrations of beams are solved using the generalized differential quadrature rule (GDQR) method to calculate the first four band gaps of each model. Investigating the influences of geometrical parameters on the band gaps shows that some bands are close to each other for specific ranges of geometrical parameters values. Furthermore, as the number of beam elements increases, the number of close band gaps increases. Having more than two close band gaps means that this periodic structure has a relatively wide band gap in total. Furthermore, this wide band can move to low frequency ranges by changing the geometrical parameters. Absorbing vibrations over a wide band gap at low frequency ranges makes this periodic structure a good vibration absorber. Verification of the analytical method using ANSYS software shows that the GDQR method can be used for vibration analysis of beam-like structures with high accuracy.

Keywords : Periodic structure; Transverse vibration; Close band gaps; GDQR method; ANSYS.

1 INTRODUCTION

VIBRATION isolation is a known technique used for reducing destructive vibrations in structures and machines. Structures with periodic geometrical and material properties have a special feature that distinguishes them from the conventional structures. They can absorb vibration waves within some frequency ranges known as vibration band gaps. The band gaps also have other applications like noise control, frequency filtering and broadband vibration energy harvesting [1, 2]. Various types of one and two-dimensional periodic structures have been introduced and analyzed in recent years [3-6]. Each periodic structure has special vibration band gap properties

*Corresponding author. Tel.: +98 3431312409, Fax.: +98 3431312202.
E-mail address: m.hajhosseini@vru.ac.ir (M. Hajhosseini)

that distinguish it from other periodic structures. Hajhosseini et al. analyzed the influences of geometrical parameters on the widths and locations of the first two band gaps of a new periodic beam model. The results obtained showed that the band gaps move to low frequency ranges and their widths increase by changing the geometrical parameters [7]. Hajhosseini and Mahdian Parrany proposed a new periodic beam-like structure. Different geometrical parameters were considered for the periodic beam and their influences on the band gaps lower and upper edges were studied. Results showed that the bands are relatively close to each other [8]. Zhu et al. studied the vibration band gap properties of a periodic lattice model consisting of zigzag beams [9]. Their results indicated that compared with the conventional triangular configuration with straight cell walls, the emerging band gaps are characterized by their upper bounding modes performing rotational deformation shapes. Wu et al. used the spectral element method to analyze the influences of material properties on the vibration band gaps of a periodic piezoelectric lattice [10]. They showed that the thickness of piezoelectric layers can affect both the energy harvesting and vibration isolation efficiencies. Various methods such as the Adomian decomposition [11], the transfer matrix [12], the lumped-mass [13], the differential quadrature [14], the lattice dynamics [15] and the finite element methods [16] were utilized to study the vibration band gap properties of different periodic structures.

In this research, a branched shape periodic structure is proposed. This structure consists of a main beam and several cantilever beams connected to this main beam by the massless and rigid links. Different number of beam elements and geometrical parameters in the form of two models are considered for this periodic structure. The generalized differential quadrature rule (GDQR) method is used to study the influences of geometrical parameters and number of beam elements on the first four band gaps. ANSYS simulations are performed to verify the analytical method and also to calculate the forced harmonic response of the periodic beam. Based on the results obtained, the main vibration band gap properties of this periodic structure are mentioned.

2 ANALYTICAL MODEL

Fig.1 shows the periodic structure introduced in this research. This figure shows that the structure consists of a main beam and several cantilever beams connected to this main beam by the massless and rigid links. The unit cell of this periodic structure is shown in Fig. 2. All beams are made of the same material. Each beam has the circular cross-section with the radius of R. The length of each beam is larger than its radius. Therefore, the Euler-Bernoulli beam theory can be applied.

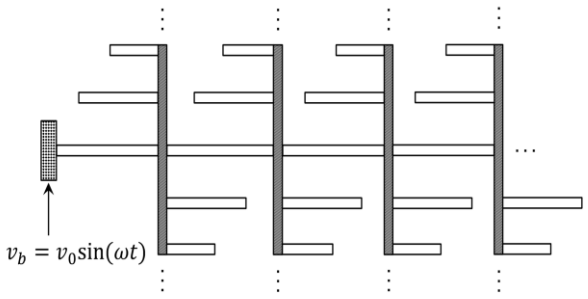

Fig.1
Branched shape periodic structure.

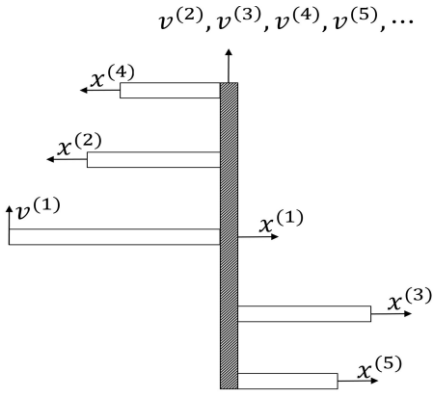

Fig.2
Unit cell.

The differential equation for free transverse vibration is written as: [17]

$$EI\frac{d^4V^{(i)}(x^{(i)})}{d\left(x^{(i)}\right)^4}=\rho A\,\omega^2V^{(i)}(x^{(i)})\ ,\ \ i=1,2,...,N_b \tag{1}$$

The slopes and transverse displacements of the beam elements must be the same at the intersection of beams. These continuity conditions are written as follows:

$$\frac{dV^{(1)}\left(L^{(1)}\right)}{dx^{(1)}}=-\frac{dV^{(i)}(0)}{dx^{(i)}},\quad i=2,4,...,N_b-1 \tag{2}$$

$$\frac{dV^{(1)}\left(L^{(1)}\right)}{dx^{(1)}}=\frac{dV^{(i)}(0)}{dx^{(i)}},\qquad i=3,5,...,N_b \tag{3}$$

$$V^{(1)}\left(L^{(1)}\right)=V^{(i)}(0),\qquad i=2,3,4,,...,N_b \tag{4}$$

At the free ends of the cantilever beams, the bending moments and axial forces are written as:

$$EI\frac{d^2V^{(i)}\left(L^{(i)}\right)}{\left(dx^{(i)}\right)^2}=0\ ,\ EI\frac{d^3V^{(i)}\left(L^{(i)}\right)}{\left(dx^{(i)}\right)^3}=0\ ,\qquad i=2,3,4,...,N_b \tag{5}$$

In order to investigate the wave propagation in a periodic structure, its unit cell is considered and Bloch–Floquet theory is applied [18]. The Bloch-periodic boundary conditions are implemented for each side of the unit cell as follows:

$$V^{(1)}\left(L^{(1)}\right)=e^{r\,k_x a}V^{(1)}(0)\ ,\ \frac{dV^{(1)}\left(L^{(1)}\right)}{dx^{(1)}}=e^{r\,k_x a}\frac{dV^{(1)}(0)}{dx^{(1)}} \tag{6}$$

$$EI\frac{d^2V^{(1)}\left(L^{(1)}\right)}{\left(dx^{(1)}\right)^2}+\sum_{i=2}^{N_b}(-1)^i\ EI\frac{d^2V^{(i)}(0)}{d\left(x^{(i)}\right)^2}=e^{r\,k_x a}EI\frac{d^2V^{(1)}(0)}{d\left(x^{(1)}\right)^2} \tag{7}$$

$$EI\frac{d^3V^{(1)}\left(L^{(1)}\right)}{\left(dx^{(1)}\right)^3}-\sum_{i=2}^{N_b}EI\frac{d^3V^{(i)}(0)}{d\left(x^{(i)}\right)^3}=e^{r\,k_x a}EI\frac{d^3V^{(1)}(0)}{d\left(x^{(1)}\right)^3} \tag{8}$$

In these equations, ρ, E, A, ω, L, I, a, N_b are the density, modulus of elasticity, cross-sectional area, angular frequency, beam length, second moment of inertia about Z axis, unit cell length and number of beam elements in each cell, respectively. Furthermore, V and r are the transverse mode shape and imaginary number, respectively. The wave vector in the x- direction is k_x .

3 NUMERICAL METHOD

The differential quadrature method (DQM) is a numerical technique used for solving the differential equations with initial or boundary conditions [19, 20, 21]. In this method, the differential equation is replaced with an algebraic

equation. Solving a set of algebraic equations is much easier than solving a set of differential equations. There are some difficulties in applying the DQM for solving the fourth-order differential equation like the governing equation of beam's transverse vibration. In this case, there is one quadrature equation in each boundary but two boundary equations are to be implemented. In order to solve this problem, the generalized differential quadrature rule method was proposed by Wu and Liu [22]. In this method, multiple degrees of freedom are defined for the boundary points. As an example, for transverse vibration of beams, the slope at each boundary is defined as a variable in addition to its displacement [23]. Before using the GDQR methods, all differential equations should be non-dimensionalized using the following non-dimensional parameters.

$$X^{(i)}=\frac{x^{(i)}}{L^{(i)}},\ Y^{(i)}=\frac{V^{(i)}}{a},\quad k=\frac{k_x\,a}{\pi},\ S^{(i)}=\frac{\rho A\,\omega^2 (L^{(i)})^4}{EI},\ \xi^{(i)}=\frac{S^{(i)}}{S^{(1)}},\qquad i=1,2,\ldots,N_b \tag{9}$$

The same grid points are used for all beams. In other words, it is assumed that $X^{(1)}=X^{(2)}=\ldots=X^{(N_b)}=X$. According to the GDQR [22], the derivatives of function $Y^{(i)}$ at the sample point X_m are defined as follows:

$$\frac{d^n Y^{(i)}(X_m)}{dX^n}=\sum_{j=1}^{N+2} D_{mj}^{(n)}\bar{Y}_j^{(i)}\quad i=1,2,\ldots,N_b\ ,\ m=1,2,\ldots\ldots,N\ ,\ n=1,2,3,4 \tag{10}$$

where

$$\left\{\bar{Y}_j^{(i)}\right\}=\left\{Y_1^{(i)},\frac{dY_1^{(i)}}{dX},Y_2^{(i)},\ldots,Y_{N-1}^{(i)},Y_N^{(i)},\frac{dY_N^{(i)}}{dX}\right\},\quad i=1,2,\ldots,N_b\ ,\ j=1,2,\ldots,N+2 \tag{11}$$

The weighting coefficients in the GDQR method are considered to be $D_{mj}^{(n)}$. Furthermore, the following function is used to determine the N grid points [24]

$$X_m=\frac{1-\cos((m-1)\pi/(N-1))}{2}\ ,\ m=1,2,\ldots,N \tag{12}$$

The differential quadrature approximation of Eq. (1) at the internal points of the i^{th} beam is written as:

$$\frac{1}{\xi^{(i)}}\sum_{j=1}^{N+2} D_{mj}^{(4)}\bar{Y}_j^{(i)}=S^{(1)}\bar{Y}_{m+1}^{(i)}\qquad m=2,3,\ldots,N-1,\ \ i=1,2,\ldots,N_b \tag{13}$$

Eqs. (2)-(8) can be expressed in the differential quadrature form as follows:

$$\bar{Y}_{N+2}^{(1)}=-\left(\frac{L^{(1)}}{L^{(i)}}\right)\bar{Y}_2^{(i)},\qquad i=2,4,\ldots,N_b-1 \tag{14}$$

$$\bar{Y}_{N+2}^{(1)}=\left(\frac{L^{(1)}}{L^{(i)}}\right)\bar{Y}_2^{(i)},\qquad i=3,5,\ldots,N_b \tag{15}$$

$$\bar{Y}_{N+1}^{(1)}=\bar{Y}_1^{(i)},\qquad i=2,3,4,\ldots,N_b \tag{16}$$

$$\frac{EI}{\left(L^{(i)}\right)^2}\sum_{j=1}^{N+2} D_{Nj}^{(2)}\bar{Y}_j^{(i)}=0\quad ,\quad \frac{EI}{\left(L^{(i)}\right)^3}\sum_{j=1}^{N+2} D_{Nj}^{(3)}\bar{Y}_j^{(i)}\quad ,\qquad i=2,3,4,\ldots,N_b \tag{17}$$

$$\bar{Y}_{N+1}^{(1)} = e^{ik\pi}\bar{Y}_1^{(1)}, \bar{Y}_{N+2}^{(1)} = e^{ik\pi}\bar{Y}_2^{(1)} \tag{18}$$

$$\sum_{j=1}^{N+2} D_{Nj}^{(2)}\bar{Y}_j^{(1)} + \sum_{i=2}^{N_b}(-1)^i\left(\frac{L^{(1)}}{L^{(i)}}\right)^2\left[\sum_{j=1}^{N+2} D_{1j}^{(2)}\bar{Y}_j^{(i)}\right] = e^{ik\pi}\sum_{j=1}^{N+2} D_{1j}^{(2)}\bar{Y}_j^{(1)} \tag{19}$$

$$\sum_{j=1}^{N+2} D_{Nj}^{(3)}\bar{Y}_j^{(1)} - \sum_{i=2}^{N_b}\left(\frac{L^{(1)}}{L^{(i)}}\right)^3\left[\sum_{j=1}^{N+2} D_{1j}^{(3)}\bar{Y}_j^{(i)}\right] = e^{ik\pi}\sum_{j=1}^{N+2} D_{1j}^{(3)}\bar{Y}_j^{(1)} \tag{20}$$

Eqs. (13)-(20) can be written in the following form

$$\begin{bmatrix} P_{dd} & P_{db} \\ P_{bd}(k) & P_{bb}(k) \end{bmatrix}\begin{pmatrix} R_d \\ R_b \end{pmatrix} = S^{(1)}\begin{pmatrix} R_d \\ 0 \end{pmatrix} \tag{21}$$

$$\begin{aligned} &\{R_d\} = \{\bar{Y}_{m+1}^{(i)}\} \\ &\{R_b\} = \{\bar{Y}_1^{(i)}, \bar{Y}_2^{(i)}, \bar{Y}_{N+1}^{(i)}, \bar{Y}_{N+2}^{(i)}\} \quad , \; i = 1,2,...,N_b \quad , \quad m = 2,3,...,N-1 \end{aligned} \tag{22}$$

Eq. (22) is rewritten as an eigenvalue problem as follow:

$$\bar{P}(k)R_d = S^{(1)}R_d \tag{23}$$

where $\bar{P}(k) = P_{dd} - P_{db}P_{bb}^{-1}(k)P_{bd}(k)$.

Solving the Eq. (23), the angular natural frequencies are calculated in terms of the wave vector k, i.e., the vibration band gaps. The wave vector is considered to be within the interval $k \in [-1, 1]$.

4 NUMERICAL EXAMPLES

A periodic beam with the unit cell length $a = L^{(1)} = 100\,mm$ is considered. The cross-sectional radius of each beam is considered to be $R = 0.5\,mm$. All beams are made of aluminum alloy with material properties $\rho = 2730\ kg/m^3$, $E = 77.56\,Gpa$. Then, two models are considered for this periodic structure. For the first model, the number of beams in each unit cell is considered to be $N_b = 3$. In this model, the beam elements 2 and 3 have the same length ($L^{(2)} = L^{(3)}$). Then, the influences of $C = L^{(2)}/L^{(1)}$ on the first four band gaps of this model are studied using the analytical method. Results are shown in Fig. 3. Fifteen grid points, $N = 15$ are used for all beams in the GDQR method.

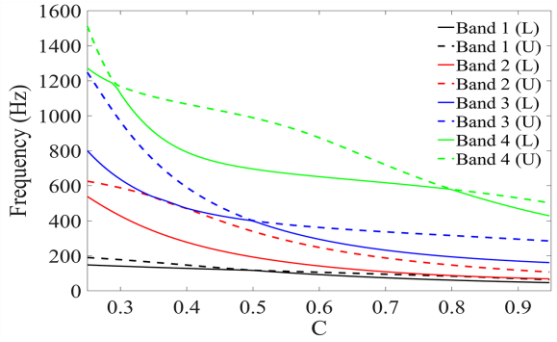

Fig.3
Effects of *C* on the band gaps of the first model.

For the second model, the number of beams is $N_b = 5$. In this model, it is assumed that $L^{(2)} = L^{(3)}$, $L^{(4)} = L^{(5)}$. The influences of C and $G = L^{(2)} - L^{(4)}$ on the first four band gaps of this model are shown in Figs. 4-6.

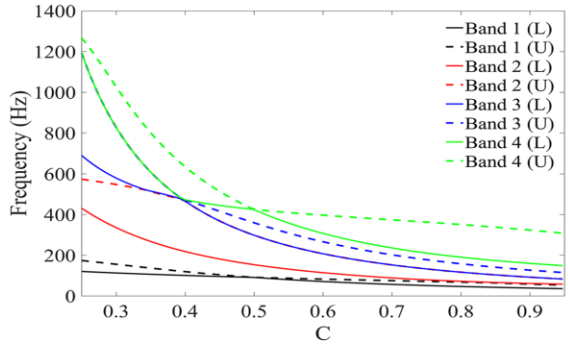

Fig.4
Effects of C on the band gaps of the second model with $G = 0$.

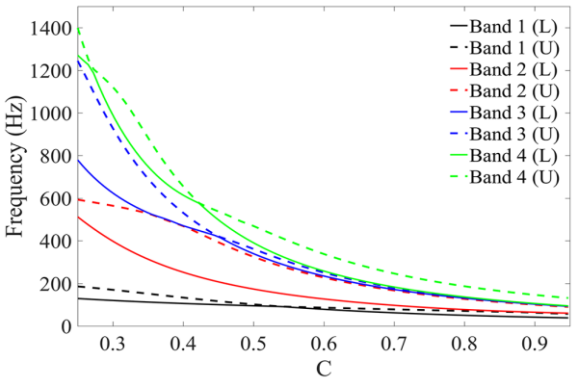

Fig.5
Effects of C on the band gaps of the second model with $G = 10mm$.

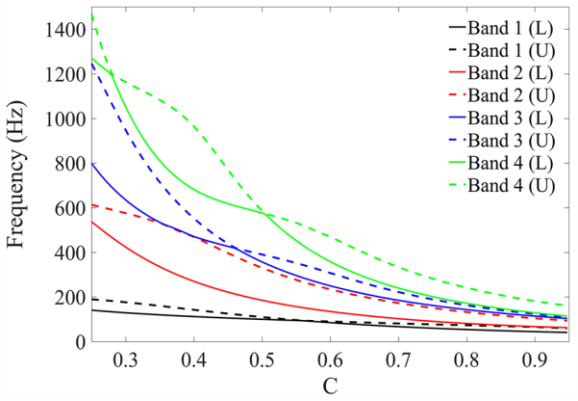

Fig.6
Effects of C on the band gaps of the second model with $G = 20mm$.

In these figures, each band's lower and upper limits are shown by L and U, respectively. Fig. 3 shows that for $N_b = 3$, the second and third bands are close to each other for $0.34 < C < 0.4$. Fig. 4 shows that for $N_b = 5$, $G = 0$, the second and third bands are close to each other for wider range of C, $0.34 < C < 0.95$. This figure also shows that the third and fourth bands of this model are close to each other for $0.25 < C < 0.4$. It can be concluded that three band gaps of this model including the second, third and fourth bands are close to each other for $0.34 < C < 0.4$. Figs 4-6 show that as G increases, these band gaps space apart from each other. Figures 3-6 show that the band gaps of each model are moved to low frequency ranges by increasing C.

The influences of C on the total width of the close band gaps of each model are shown in Figs. 7-10. Comparing Figs. 7 and 10 shows that the total width of three close bands of the second model with $G = 0$ is larger than the total width of two close band gaps of the first model.

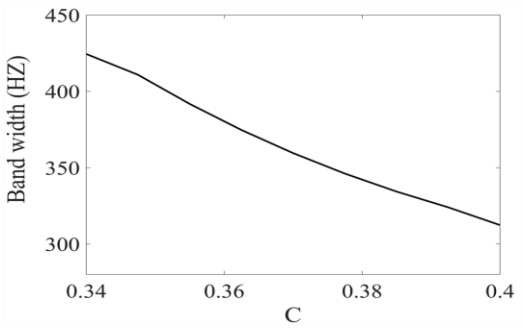

Fig.7
Effects of C on the total width of the second and third bands for $N_b = 3$.

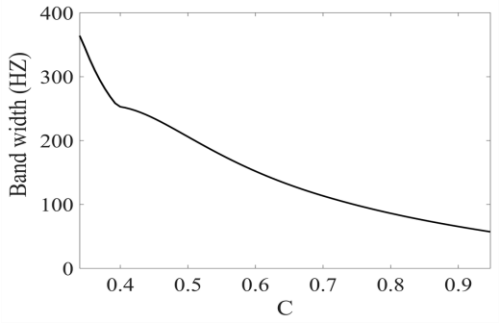

Fig.8
Effects of C on the total width of the second and third bands for $N_b = 5, G = 0$.

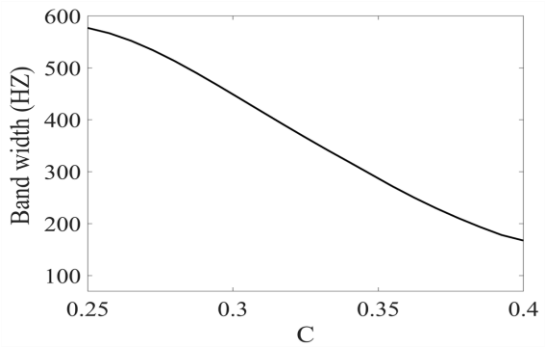

Fig.9
Effects of C on the total width of the third and fourth bands for $N_b = 5, G = 0$.

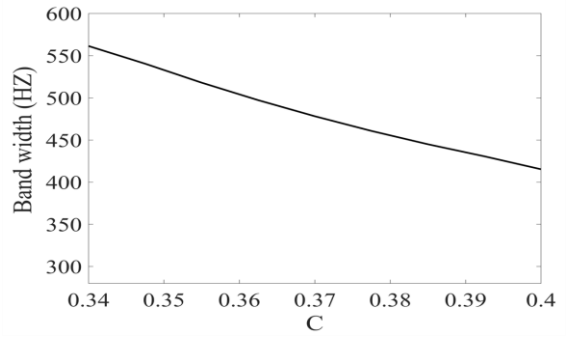

Fig.10
Effects of C on the total width of the second, third and fourth bands for $N_b = 5, G = 0$.

5 FINITE ELEMENT SIMULATION

In this section, a periodic beam with $a = L^{(1)} = 100mm$ and seven-unit cells is considered. Aluminum alloy is used for all beams. Then, four models with different geometrical parameters are designed and meshed in the ANSYS software. The beams are designed as straight lines. These lines are meshed using BEAM189 element. The BEAM189 element is used to analyze slender beam elements. This element is a quadratic three-node beam element

having six degrees of freedom at each node. The Sections command is used to define the shape of the cross-section and its relevant geometrical parameters. After meshing, the CE command is used to apply the constraint equations generated by the massless and rigid links. As an example, a model with the geometrical parameters $N_b = 5$, $C = 0.7$, $G = 20mm$ is considered. Fig. 11 shows the finite element model.

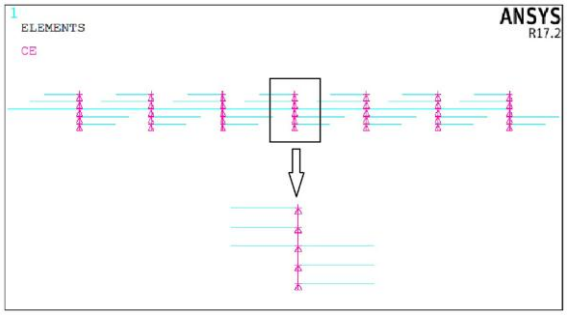

Fig.11
Finite element model for $N_b = 5$, $C = 0.7$, $G = 20mm$.

As shown in Fig. 1, for each finite element model, the cantilever end of the periodic structure is subjected to a harmonic motion in the Y direction. This motion has the amplitude of $v_0 = 0.1mm$. Then, the forced harmonic responses of these four finite element models are calculated using the ANSYS. Results are shown in Figs. 12(b)-15(b). In these figures, the forced vibration responses of the second, fifth and seventh cells are plotted in terms of frequency. Figs. 12(b)-15(b) show that within frequency ranges shown by gray color, the amplitudes of vibration decrease as the cells distance from the excitation point. In other words, the vibration waves are forbidden from propagation in this periodic beam. These frequency ranges are vibration band gaps. Furthermore, the analytical method is used to calculate the band gaps of these finite element models. Results are shown in Figs. 12(a)-15(a). These figures show that there is no wave vector or wave propagation for some frequency ranges. These frequency ranges are also vibration band gaps and shown by gray color.

Comparing part (a) and (b) in Figs. 12-15, indicates a good matching between the analytical results and FEM ones. In order to show this better, the band gaps lower and upper limits calculated by these two methods are represented in Tables 1 and 2.

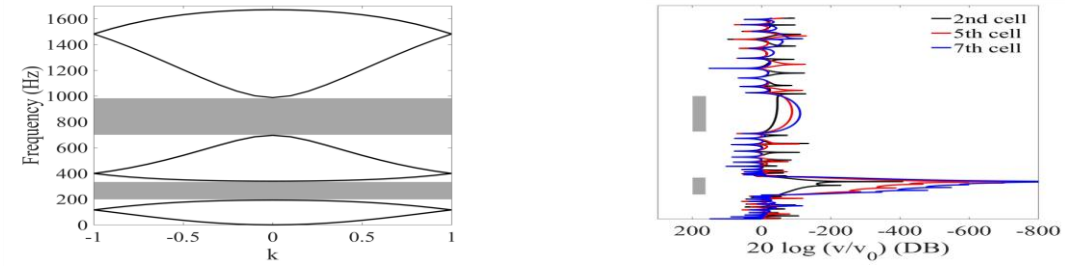

(a) (b)

Fig.12
Band gaps of the first model with $C = 0.5$ obtained from: (a) GDQR, (b) ANSYS.

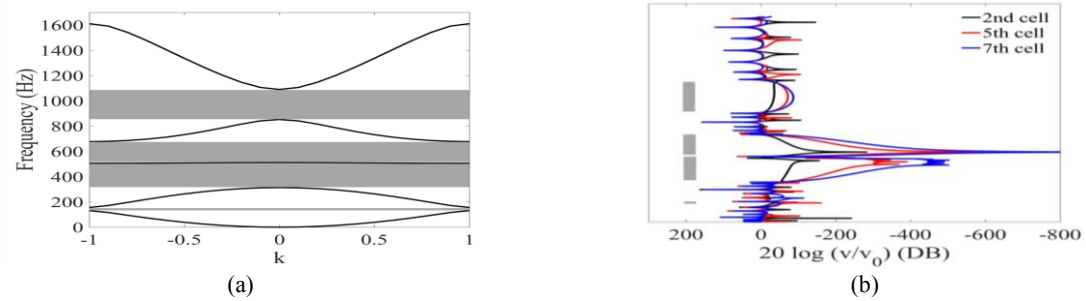

(a) (b)

Fig.13
Band gaps of the first model with $C = 0.37$ obtained from: (a) GDQR, (b) ANSYS.

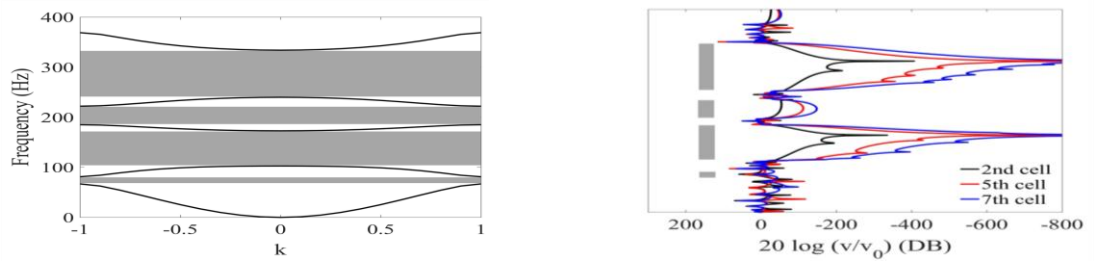

(a) (b)

Fig.14
Band gaps of the second model with $C = 0.7, G = 20mm$ obtained from: (a) GDQR, (b) ANSYS.

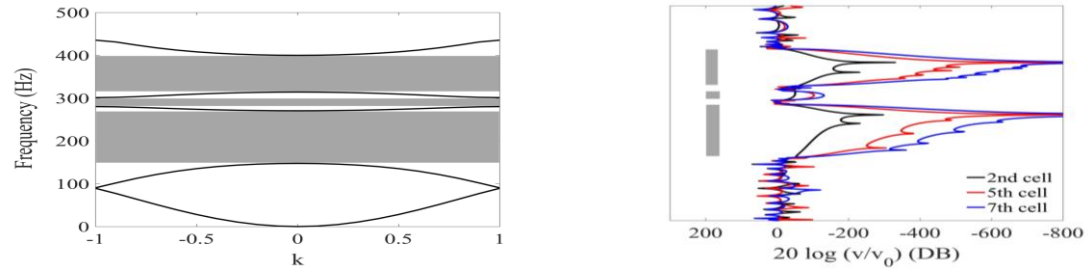

(a) (b)

Fig.15
Band gaps of the second model with $C = 0.55, G = 10mm$ obtained from: (a) GDQR, (b) ANSYS.

Table 1
The first four band gaps of the first model.

C	Method	First band	Second band	Third band	Fourth band
0.5	GDQR	No band	192 – 338	No band	695 – 988
	FEM	No band	193 – 337	No band	689 – 982
0.37	GDQR	131 – 156	313 – 506	510 – 677	852 – 1090
	FEM	125 – 149	313 – 505	511 – 676	850 – 1087

Table 2
The first four band gaps of the second model.

C	G (mm)	Method	First band	Second band	Third band	Fourth band
0.7	20	GDQR	66 – 81	102 – 172	184 – 222	239 – 333
		FEM	67 – 84	103 – 173	185 – 220	240 – 334
0.55	10	GDQR	No band	147 – 270	280 – 301	314 – 400
		FEM	No band	148 – 271	281 – 300	315 – 399

In order to show the wave propagation within the band gaps, as an example, the periodic beam with $N_b = 5$, $C = 0.7$, $G = 20mm$ is considered. Then, the ANSYS software is used to calculate the forced harmonic response at the frequency $f = 137Hz$. This frequency is in the second band gap. Result is shown in Fig. 16.

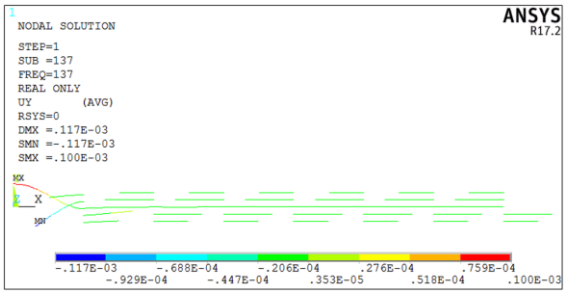

Fig.16
Forced harmonic response.

6 CONCLUSION

A new periodic structure composed of a main beam and several cantilever beams connected to the main beam is proposed. Different number of beams and geometrical parameters in the form of two models are considered for this periodic structure. The GDQR method is used to study the influences of geometrical parameters on the locations and widths of the first four band gaps. Results show that some bands are attached to each other for specific ranges of geometrical parameters values. Furthermore, the number of close band gaps increases when the number of beams increases. Having more than two close band gaps means that this periodic structure has a relatively wide band gap in total. The location of this wide band gap can be changed by changing the geometrical parameters. Absorbing transverse vibrations over a wide band gap at low frequency ranges makes the proposed periodic structure a good vibration absorber for practical applications. The numerical method used in this study is found to be precisely applicable to the vibration analysis of beam-like structures.

REFERENCES

[1] Hajhosseini M., Rafeeyan M., 2016, Modeling and analysis of piezoelectric beam with periodically variable cross-sections for vibration energy harvesting, *Applied Mathematics and Mechanics* **37**(8): 1053-1066.

[2] Wen J.H., Wang G., Yu D.L., Zhao H.G., Liu Y.Z., 2008, Study on the vibration band gap and vibration attenuation property of phononic crystals, *Science in China Series E-Technological Sciences* **51**(1): 85-99.

[3] Olhoff N., Niu B., Cheng G., 2012, Optimum design of band-gap beam structures, *International Journal of Solids and Structures* **49**(22): 3158-3169.

[4] Kamotski L.V., Smyshlyaev V.P., 2019, Band gaps in two-dimensional high-contrast periodic elastic beam lattice materials, *Journal of the Mechanics and Physics of Solids* **123**: 292-304.

[5] Xiang H.J., Cheng Z.B., Shi Z.F., Yu X.Y., 2014, In-plane Band Gaps in a Periodic Plate with Piezoelectric Patches, *Journal of Solid Mechanics* **6**(2): 194-207.

[6] Zouari S., Brocail J., Génevaux J.M., 2018, Flexural wave band gaps in metamaterial plates: A numerical and experimental study from infinite to finite models, *Journal of Sound and Vibration* **435**: 246-263.

[7] Hajhosseini M., Rafeeyan M., Ebrahimi S., 2017, Vibration band gap analysis of a new periodic beam model using GDQR method, *Mechanics Research Communications* **79**: 43-50.

[8] Hajhosseini M., Mahdian Parrany A., 2019, Vibration band gap properties of a periodic beam-like structure using the combination of GDQ and GDQR methods, *Waves in Random and Complex Media* **2019**: 1-17.

[9] Zhu Z.W., Deng Z.C., Huang B., Du J.K., 2019, Elastic wave propagation in triangular chiral lattices: Geometric frustration behavior of standing wave modes, *International Journal of Solids and Structures* **158**: 40-51.

[10] Wu Z.J., Li F.M., Zhang C., 2014, Vibration properties of piezoelectric square lattice structures, *Mechanics Research Communications* **62**: 123-131.

[11] Hajhosseini M., Ebrahimi S., 2019, Analysis of vibration band gaps in an Euler–Bernoulli beam with periodic arrays of meander-shaped beams, *Journal of Vibration and Control* **25**(1): 41-51.

[12] Guo X., Liu H., Zhang K., Duan H., 2018, Dispersion relations of elastic waves in two-dimensional tessellated piezoelectric phononic crystals, *Applied Mathematical Modelling* **56**: 65-82.

[13] Wang G., Wen J., Liu Y., Wen X., 2004, Lumped-mass method for the study of band structure in two-dimensional phononic crystals, *Physical Review B - Condensed Matter and Materials Physics* **69**: 184302.

[14] Liang X., Wang T., Jiang X., Liu Z., Ruan Y., Deng Y., 2019, A numerical method for flexural vibration band gaps in a phononic crystal beam with locally resonant oscillators, *Crystals* **9**(6): 293.

[15] Chang I.L., Liang Z.X., Kao H.W., Chang S.H., Yang C.Y., 2018, The wave attenuation mechanism of the periodic local resonant metamaterial, *Journal of Sound and Vibration* **412**: 349-359.

[16] Zhou X., Xu Y., Liu Y., Lv L., Peng F., Wang L., 2018, Extending and lowering band gaps by multilayered locally resonant phononic crystals, *Applied Acoustics* **133**: 97-106.

[17] Leissa A.W., Qatu M.S., 2011, *Vibration of Continuous Systems*, McGraw-Hill Professional.

[18] Kittel C., 2005, *Introduction to Solid State Physics*, John Wiley & Sons, New York.

[19] Bellman R., Casti J., 1971, Differential quadrature and long-term integration, *Journal of Mathematical Analysis and Applications* **34**(2): 235-238.

[20] Liang X., Zha X., Jiang X., Cao Z., Wang Y., Leng J., 2019, A semi-analytical method for the dynamic analysis of cylindrical shells with arbitrary boundaries, *Ocean Engineering* **178**: 145-155.

[21] Liang X., Deng Y., Jiang X., Cao Z., Ruan Y., Leng J., Wang T., Zha X., 2019, Three-dimensional semi-analytical solutions for the transient response of functionally graded material cylindrical panels with various boundary conditions, *Journal of Low Frequency Noise, Vibration and Active Control* **39**: 1002-1023.

[22] Wu T.Y., Liu G.R., 1999, A differential quadrature as a numerical method to solve differential equations, *Computational Mechanics* **24**(3): 197-205.

[23] Hajhosseini M., 2020, Analysis of complete vibration bandgaps in a new periodic lattice model using the differential quadrature method, *Journal of Vibration and Control* **26**: 1708-1720.
[24] Shu C., 2000, *Differential Quadrature and its Applications in Engineering*, Springer-Verlag, London.